Magnetic Nanoparticles

DOI: 10.1002/anie.200800014

Multifunctional Nanoparticles Displaying Magnetization and Near-IR Absorption**

*Leyu Wang, Jingwei Bai, Yujing Li, and Yu Huang**

Nanoparticles are attracting considerable interest in biomedical research owing to their significant potential to offer new opportunities for early diagnosis and therapeutics. For example, magnetic nanoparticles[1–3] have been widely investigated in the application of magnetic resonance imaging (MRI),[4,5] magnetic bioseparation,[6–8] and targeted drug/gene delivery.[9–11] Furthermore, nanoparticle-mediated photothermal ablation therapy,[12] in which nanoparticles absorb radiation and convert it into thermal energy to kill nearby malignant cells, is also drawing increasing attention for cancer therapy owing to the minimally invasive nature of the procedure compared to conventional surgery, relatively simple operation, as well as short recovery times and reduced complication rates.[13] Among various forms of photothermal ablation technologies, near-infrared (NIR) absorption photothermal therapy is particularly interesting because of the low scattering and low absorption by blood and soft tissue in this spectral region and the resulting lower extent of collateral damage.[13,14] The combination of MRI diagnosis, targeted delivery, and NIR photothermal ablation would greatly increase the treatment efficacy and simultaneously minimize the damage to normal cells and tissues. Herein, we demonstrated the synthesis of Fe_3O_4@polymer@Au shell multifunctional nanoparticles that display both magnetism and NIR absorption. The as-prepared nanoparticles can simultaneously offer promising possibilities for movement control using an external magnetic field to direct the nanoparticles to cancer tumors, MRI imaging diagnosis, as well as strong NIR absorption for photothermal ablation.

Over the past few years, owing to the biocompatible surface and novel optical properties of gold nanostructures,[15] many research efforts have been focused on developing gold nanostructures to exploit these properties,[16,17] especially regarding surface plasmon resonance (SPR) in the NIR region[13,14,18–24] for biomedical applications. To date, gold nanocages,[14,19] nanorods,[23,24] nanorings,[25] and polymer-supported gold nanoshells[13,20–22] with NIR absorption have been synthesized, and their application in photothermal ablation of cancer cells and tissues has been demonstrated. Recently, magnetic-core gold-shell nanoparticles have captured particular attention, owing to the combined functions of magnetic and optical properties from the two components, which can lead to exciting opportunities for integrated imaging, diagnosis, targeted drug delivery, and therapeutics.[20,26,27] A few examples have been reported that combine the NIR optical properties of gold with magnetic properties. However, the reported nanoparticles either form aggregates with gold coatings, that is, do not form individual core–shell nanostructure, or have magnetization too low to be directed by an external magnetic field.[20,26,27] To our knowledge, it remains a grand challenge to develop magnetic, NIR-absorptive bifunctional gold-shell nanostructures to facilitate targeted delivery and MRI diagnosis while retaining a strong NIR absorption. Herein, we report a new class of potential photothermal therapeutic agents based on gold-shell-coated magnetite nanoparticles. In brief, as shown in Scheme 1,

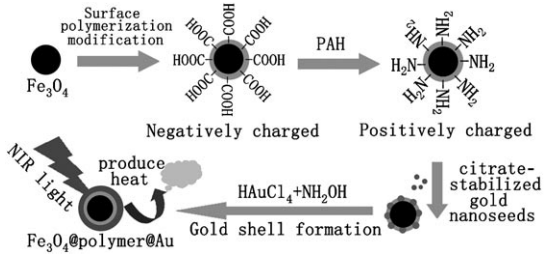

Scheme 1. Schematic depiction of the fabrication of Fe_3O_4@polymer@Au shell core–shell nanostructure. PAH = poly(allylamine hydrochloride).

magnetite nanoparticles[28] were prepared with a thin polymer coating,[29] and gold nanoshells were then introduced to form the core–shell nanostructure. It is important to note that direct coating of magnetic nanoparticles with gold nanoshells does not produce NIR absorption (see the Supporting Information, Figure S1), which is consistent with similar structures reported previously.[30,31] Therefore, the polymer shell here, although very thin, is believed to help maintain the NIR absorption of the gold nanoshell, possibly by interrupting the interactions between the gold shell and the magnetite core.

Magnetite nanoparticles were synthesized in ethylene glycol through a solvothermal method using $FeCl_3 \cdot 6H_2O$ as the single iron source and CH_3COONa as alkali.[28] As shown in Figure 1a, the magnetite nanoparticles have a relatively smooth surface and an average diameter of 258 ± 18.7 nm. A thin layer of polymer shell was then formed in situ through

[*] Dr. L. Wang, J. Bai, Y. Li, Prof. Y. Huang
Department of Materials Science and Engineering
University of California
Los Angeles, CA 90095 (USA)
Fax: (+1) 310-206-7353
E-mail: yhuang@seas.ucla.edu

[**] This work was supported by UCLA new faculty start-up fund and UCLA Henry Samuli School of Applied Science and Engineering Fellowship.

Supporting information for this article is available on the WWW under http://www.angewandte.org or from the author.

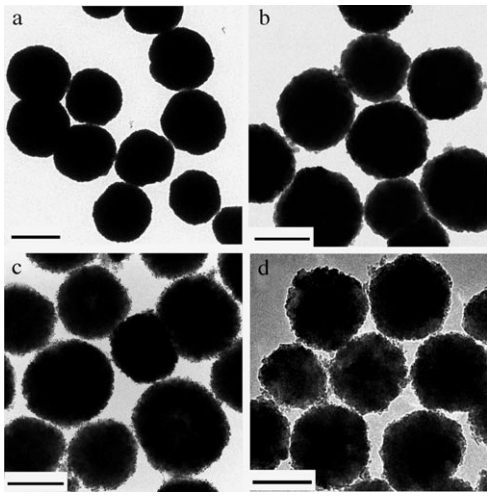

Figure 1. TEM images of the as-prepared nanoparticles. a) Fe_3O_4 core; b) Fe_3O_4@polymer; c) Fe_3O_4@polymer@Au seeds; d) Fe_3O_4@polymer@Au shell. The scale bar is 200 nm in all images. A larger version of (d) is shown in the Supporting Information (Figure S3).

copolymerization of methacrylic acid and acrylamide.[29] The surface of the nanoparticles appeared rougher after polymer coating (Figure 1 b). The thickness of the polymer shell can be tuned by varying the monomer concentration. Higher monomer concentrations usually lead to thicker polymer shells. A thin polymer shell is preferred in this case, as thicker polymer shells usually cause aggregation of magnetic nanoparticles (see the Supporting Information, Figure S2), making it hard to achieve individual core–shell nanoparticle structures. It should be pointed out that this thin layer of polymer is enough to retain the NIR absorption of the gold nanoshells. After the formation of the copolymer shell, the nanoparticle surface is negatively charged owing to the carboxy groups introduced by methacrylic acid. The copolymer surface was coated with another thin layer of positively charged polyelectrolyte, poly(allylamine hydrochloride) (PAH) through electrostatic interaction.[32] PAH introduces amine groups to the nanoparticle surface, which in turn render a positively charged surface for electrostatic attachment of gold seeds, which were stabilized in solution by negatively charged citrate groups.[33] As shown in Figure 1 c, the gold seeds can be clearly seen on the polymer-coated magnetite surface. After attachment of gold seeds, the gold nanoshell was formed by selectively reducing gold onto the surface of the gold seeds through a surface catalytic reaction using chloroauric acid ($HAuCl_4 \cdot 3H_2O$, 1.0 wt %) and hydroxylamine hydrochloride ($NH_2OH \cdot HCl$, 80 mM; see the Experimental Section).[34] Repeated reductive deposition led to a continuous gold nanoshell. Note that all the reducing reactions were conducted under ultrasonication in an ice bath. The ultrasonication helps prevent the magnetic nanoparticles from aggregating because of the magnetic interactions. However, at the same time, ultrasonication increases the system temperature as well as the reaction rate, which would lead to aggregation of the particles and a roughened gold-shell surface. The ice bath is necessary to maintain a lower temperature and hence a lower reaction rate to achieve a smooth gold coating. Furthermore, the ice bath could also help diminish nanoparticle aggregation resulting from the elevated temperature caused by ultrasonication. The TEM image of the as-made Fe_3O_4@polymer@Au shell core–shell nanostructures shows well-separated individual nanoparticle structures with smooth gold shells with an average diameter of 273 ± 17.9 nm (Figure 1 d).

The formation of the Fe_3O_4@polymer@Au shell core–shell nanostructures was further characterized by Fourier transform infrared (FTIR) spectroscopy, X-ray powder diffraction (XRD), and energy dispersive X-ray (EDX) spectroscopy (see the Supporting Information, Figures S4–S6). The FTIR spectroscopy results of the polymer-coated nanoparticles indicated the existence of the polymer coating, showing strong absorption peaks (see Figure S4 in the Supporting Information). The intensity of the absorption peaks of the polymer layer greatly decreased with the formation of the gold shell, which further confirms the formation of the gold nanoshell on the existing polymer surface. The XRD pattern of the magnetic nanoparticles is identical to that of cubic-phase magnetite. After the formation of the gold shell, gold peaks appeared in the XRD pattern (see the Supporting Information, Figure S5). EDX spectroscopy analysis further confirmed the existence of the gold nanoshell on the surface of the magnetite nanoparticles (see the Supporting Information, Figure S6).

UV/visible absorption spectroscopy experiments were carried out to confirm that the as-prepared core–shell nanoparticles display the NIR absorption of the gold nanoshells (Figure 2). All nanoparticles were dispersed in deionized water for absorption experiments. The gold-coated magnetite nanoparticles were modified with thiolated poly(ethylene glycol) (PEG) to increase their hydrophilicity and to maintain a stable colloidal suspension. From Figure 2, it is clear that the absorption spectrum of polymer-coated magnetite nanoparticles shows an absorption peak around 540 nm without absorption in the NIR region (curve 1). After attaching the gold seeds to the polymer surface (curve 2), the peak position red shifted slightly; however, still no obvious NIR absorption was observed. When gold was further reduced onto the existing surface of the gold seeds to form more complete gold nanoshells (see the Experimental Section), the absorption in the NIR range started to appear (Figure 2, curves 3–5). Curves 3, 4, and 5 show the absorption spectra of the core–shell nanoparticles after a first, second, and third round of gold-reducing reaction, respectively (see the Experimental Section). With the formation of gold nanoshells, the maximum absorption peak red shifted and the NIR absorption increased step by step, consistent with previous studies.[35,36] The change in the absorption spectra is also reflected in the colors of the colloidal suspensions of the nanoparticles. Figure 2 b shows how the colors of the Fe_3O_4@polymer, Fe_3O_4@polymer@Au seeds, and Fe_3O_4@polymer@Au shell colloidal solutions change from brown to dark brown and finally to dark blue with the formation of the Au nanoshells. This picture also demonstrates the uniformity and stability of the as-made core–shell nanoparticles in aqueous solution, which is important for biomedical applications.

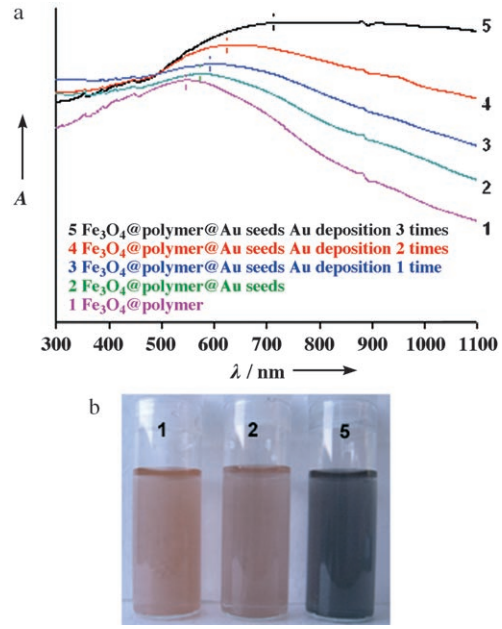

Figure 2. a) NIR absorption spectra. Curve 1: Fe_3O_4@polymer nanoparticles; curve 2: Fe_3O_4@polymer@Au seeds nanoparticles; curve 3: Fe_3O_4@polymer@Au shell after first round of gold deposition; curve 4: Fe_3O_4@polymer@Au shell after second round of Au deposition; curve 5: Fe_3O_4@polymer@Au shell after third round of Au deposition. b) Photographs of the nanoparticle solutions in sunlight. See the Experimental Section for synthesis details. The concentration of the nanoparticle suspension is about 0.2 mg mL^{-1} (for Fe_3O_4 core).

The magnetic properties of the as-prepared magnetite core and the Fe_3O_4@polymer@Au shell core–shell nanostructure were studied using a superconducting quantum interference device (SQUID) magnetometer at room temperature. The plots of magnetization versus magnetic field (M–H loop) at 25 °C are illustrated in Figure 3. The M–H loops show that both nanoparticles have fairly strong magnetization and that the saturation magnetization (M_s) is 75.6 emu g^{-1} and 61.0 emu g^{-1} for the Fe_3O_4 core and Fe_3O_4@polymer@Au shell core–shell nanostructure, respectively. The decrease in M_s may be attributed to the increased mass of the nanoparticle introduced by the gold nanoshell. The strong magnetization of the nanoparticles was also revealed by the fact that they were easily attracted by an external magnetic field (Figure 4). The strong magnetization of these core–shell nanoparticles should facilitate MRI and targeted delivery applications.

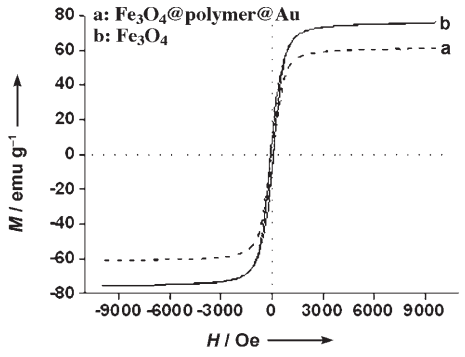

Figure 3. Room-temperature magnetization curves of a) Fe_3O_4@polymer@Au shell and b) Fe_3O_4 core nanoparticles.

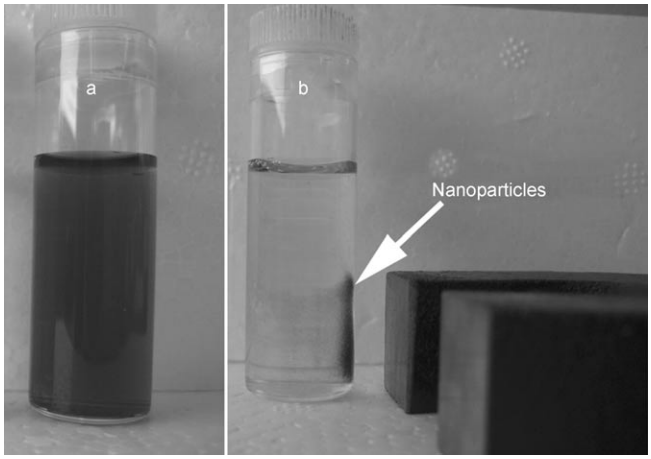

Figure 4. Photographs of the Fe_3O_4@polymer@Au shell nanoparticle colloidal solution before (a) and after (b) magnetic separation by an external magnetic field. The arrow highlights the nanoparticles that were attracted to the side of the vial by a magnet.

In conclusion, we have synthesized multifunctional Fe_3O_4@polymer@Au shell core–shell nanoparticle structures with good dispersibility and stability in aqueous solution. Our studies demonstrate that both the strong magnetization of the magnetite core and the NIR optical absorption of the gold nanoshell are retained in this multifunctional nanoparticle structure. The combined functionalities will open up many exciting opportunities in biomedical applications, such as integrated imaging, diagnosis, targeted delivery, and therapeutics.

Experimental Section

Polymer coating of magnetite nanoparticles: The characterization and preparation of gold nanoseeds are described in the Supporting Information. The magnetite nanoparticles were prepared according to the procedure published by Li and co-workers.[28] Then, the as-prepared magnetite nanoparticle colloidal solution (2 mL, 10 mg mL^{-1} in ethanol), methacrylic acid (30 mg), acrylamide (30 mg), ethylene glycol dimethacrylate (EGDMA, 20 mg), and 2,2′-azobis(2-methylpropionitrile) (25 mg) as initiator were dispersed in acetonitrile (40 mL) and ultrasonicated for 10 min. Then the mixture solution was heated to boiling for 2 h. During the boiling process, occasional ultrasonication was used to prevent the nanoparticles from aggregating. The polymer-coated nanoparticles were magnetically purified with an external magnetic field and washed with ethanol and with water (three times). Then the nanoparticles were dispersed in water (4 mL) to form a solution (5 mg mL^{-1} for Fe_3O_4 core) and stored for use.

PAH coating of Fe_3O_4@polymer nanoparticles: The above Fe_3O_4@polymer nanoparticle solution (1.0 mL) was injected into water (20 mL) and ultrasonicated for 5 min in an ice bath. Thereafter, $NH_3 \cdot H_2O$ (28–30 wt %, 20 μL) was added to produce a weakly basic solution (pH 8.5). Then aqueous poly(allylamine hydrochloride) (PAH, 10 mg mL^{-1}, 20 μL) was introduced and the mixture was ultrasonicated for 15 minutes in an ice bath. Finally, the nanoparticles were purified by external magnetic field and washed with water three

times. The PAH-modified nanoparticles were dispersed in water (20 mL) for subsequent experiments.

Gold seeds coating: The as-prepared gold nanoparticle colloidal solution (20 mL) was added to the Fe_3O_4@polymer@PAH nanoparticle colloidal solution prepared above (20 mL). The mixture was ultrasonicated for 15 minutes in an ice bath. Owing to the electrostatic interaction, the gold nanoparticles were absorbed onto the surface of PAH-modified magnetite nanoparticles. Thereafter, the nanoparticles were purified by external magnetic field and washed with water three times. The gold-seed-modified magnetite nanoparticles were dispersed in water (20 mL). Subsequently, thiolated PEG (5 mg) was added, and the solution was ultrasonicated for ten minutes. The thiolated-PEG-modified nanoparticles were then purified and washed with water three times. The resulting thiolated-PEG-modified Fe_3O_4@polymer@Au seeds nanoparticles were dispersed into deionized water (40 mL) under ultrasonication.

Gold shell formation: Chloroauric acid solution ($HAuCl_4 \cdot 3H_2O$, 1.0 wt%, 50 μL) was added to the thiolated-PEG-modified Fe_3O_4@polymer@Au seeds nanoparticle solution (40 mL) and ultrasonicated for 2 min. Then hydroxylamine solution (80 mM, 100 μL) was introduced and the ultrasonication was continued for 15 minuntes in an ice bath. The core–shell nanoparticles were separated with an external magnetic field and washed with water at least three times. Then the particles were dispersed into water (20 mL) under ultrasonication, and thiolated PEG (5 mg) was added to modify the surface. The surface-modification reaction with PEG was allowed to proceed for 10 minutes. Then the particles were purified as described above. This gold deposition and purification procedure was repeated one to three times to form the continuous gold nanoshell.

Received: January 3, 2008
Published online: February 15, 2008

Keywords: gold · magnetic properties · nanostructures · NIR absorption · photothermal ablation

[1] R. Hong, N. O. Fischer, T. Emrick, V. M. Rotello, *Chem. Mater.* **2005**, *17*, 4617.
[2] J. P. Ge, Y. X. Hu, Y. D. Yin, *Angew. Chem.* **2007**, *119*, 7572; *Angew. Chem. Int. Ed.* **2007**, *46*, 7428.
[3] J. P. Ge, Y. X. Hu, M. Biasini, W. P. Beyermann, Y. D. Yin, *Angew. Chem.* **2007**, *119*, 4420; *Angew. Chem. Int. Ed.* **2007**, *46*, 4342.
[4] W. S. Seo, J. H. Lee, X. M. Sun, Y. Suzuki, D. Mann, Z. Liu, M. Terashima, P. C. Yang, M. V. McConnell, D. G. Nishimura, H. J. Dai, *Nat. Mater.* **2006**, *5*, 971.
[5] M. Lewin, N. Carlesso, C. H. Tung, X. W. Tang, D. Cory, D. T. Scadden, R. Weissleder, *Nat. Biotechnol.* **2000**, *18*, 410.
[6] H. W. Gu, P. L. Ho, K. W. T. Tsang, L. Wang, B. Xu, *J. Am. Chem. Soc.* **2003**, *125*, 15702.
[7] H. W. Gu, K. M. Xu, C. J. Xu, B. Xu, *Chem. Commun.* **2006**, 941.
[8] L. Y. Wang, J. Bao, L. Wang, F. Zhang, Y. D. Li, *Chem. Eur. J.* **2006**, *12*, 6341.
[9] J. R. McCarthy, K. A. Kelly, E. Y. Sun, R. Weissleder, *Nanomedicine* **2007**, *2*, 153.
[10] S. Giri, B. G. Trewyn, M. P. Stellmaker, V. S. Y. Lin, *Angew. Chem.* **2005**, *117*, 5166; *Angew. Chem. Int. Ed.* **2005**, *44*, 5038.
[11] T. J. Yoon, J. S. Kim, B. G. Kim, K. N. Yu, M. H. Cho, J. K. Lee, *Angew. Chem.* **2005**, *117*, 1092; *Angew. Chem. Int. Ed.* **2005**, *44*, 1068.
[12] M. Kettering, J. Winter, M. Zeisberger, S. Bremer-Streck, H. Oehring, C. Bergemann, C. Alexiou, R. Hergt, K. J. Halbhuber, W. A. Kaiser, I. Hilger, *Nanotechnology* **2007**, *18*, 175101.
[13] L. R. Hirsch, R. J. Stafford, J. A. Bankson, S. R. Sershen, B. Rivera, R. E. Price, J. D. Hazle, N. J. Halas, J. L. West, *Proc. Natl. Acad. Sci. USA* **2003**, *100*, 13549.
[14] J. Y. Chen, D. L. Wang, J. F. Xi, L. Au, A. Siekkinen, A. Warsen, Z. Y. Li, H. Zhang, Y. N. Xia, X. D. Li, *Nano Lett.* **2007**, *7*, 1318.
[15] R. Hong, G. Han, J. M. Fernandez, B. J. Kim, N. S. Forbes, V. M. Rotello, *J. Am. Chem. Soc.* **2006**, *128*, 1078.
[16] X. Y. Xu, M. S. Han, C. A. Mirkin, *Angew. Chem.* **2007**, *119*, 7572; *Angew. Chem. Int. Ed.* **2007**, *46*, 3468.
[17] J. S. Lee, M. S. Han, C. A. Mirkin, *Angew. Chem.* **2007**, *119*, 4171; *Angew. Chem. Int. Ed.* **2007**, *46*, 4093.
[18] F. Kim, S. Connor, H. Song, T. Kuykendall, P. D. Yang, *Angew. Chem.* **2004**, *116*, 3759; *Angew. Chem. Int. Ed.* **2004**, *43*, 3673.
[19] J. Y. Chen, B. Wiley, Z. Y. Li, D. Campbell, F. Saeki, H. Cang, L. Au, J. Lee, X. D. Li, Y. N. Xia, *Adv. Mater.* **2005**, *17*, 2255.
[20] X. J. Ji, R. P. Shao, A. M. Elliott, R. J. Stafford, E. Esparza-Coss, J. A. Bankson, G. Liang, Z. P. Luo, K. Park, J. T. Markert, C. Li, *J. Phys. Chem. C* **2007**, *111*, 6245.
[21] C. Loo, A. Lowery, N. Halas, J. West, R. Drezek, *Nano Lett.* **2005**, *5*, 709.
[22] A. M. Gobin, M. H. Lee, N. J. Halas, W. D. James, R. A. Drezek, J. L. West, *Nano Lett.* **2007**, *7*, 1929.
[23] C. C. Chen, Y. P. Lin, C. W. Wang, H. C. Tzeng, C. H. Wu, Y. C. Chen, C. P. Chen, L. C. Chen, Y. C. Wu, *J. Am. Chem. Soc.* **2006**, *128*, 3709.
[24] X. H. Huang, I. H. El-Sayed, W. Qian, M. A. El-Sayed, *J. Am. Chem. Soc.* **2006**, *128*, 2115.
[25] E. M. Larsson, J. Alegret, M. Kall, D. S. Sutherland, *Nano Lett.* **2007**, *7*, 1256.
[26] J. Kim, S. Park, J. E. Lee, S. M. Jin, J. H. Lee, I. S. Lee, I. Yang, J. S. Kim, S. K. Kim, M. H. Cho, T. Hyeon, *Angew. Chem.* **2006**, *118*, 7918; *Angew. Chem. Int. Ed.* **2006**, *45*, 7754.
[27] V. Salgueirino-Maceira, M. A. Correa-Duarte, M. Farle, A. Lopez-Quintela, K. Sieradzki, R. Diaz, *Chem. Mater.* **2006**, *18*, 2701.
[28] H. Deng, X. L. Li, Q. Peng, X. Wang, J. P. Chen, Y. D. Li, *Angew. Chem.* **2005**, *117*, 2842; *Angew. Chem. Int. Ed.* **2005**, *44*, 2782.
[29] F. Bai, X. L. Yang, R. Li, B. Huang, W. Q. Huang, *Polymer* **2006**, *47*, 5775.
[30] Z. C. Xu, Y. L. Hou, S. H. Sun, *J. Am. Chem. Soc.* **2007**, *129*, 8698.
[31] T. A. Larson, J. Bankson, J. Aaron, K. Sokolov, *Nanotechnology* **2007**, *18*, 325101.
[32] L. Y. Wang, R. X. Yan, Z. Y. Hao, L. Wang, J. H. Zeng, H. Bao, X. Wang, Q. Peng, Y. D. Li, *Angew. Chem.* **2005**, *117*, 6208; *Angew. Chem. Int. Ed.* **2005**, *44*, 6054.
[33] K. R. Brown, A. P. Fox, M. J. Natan, *J. Am. Chem. Soc.* **1996**, *118*, 1154.
[34] J. L. Lyon, D. A. Fleming, M. B. Stone, P. Schiffer, M. E. Williams, *Nano Lett.* **2004**, *4*, 719.
[35] E. Prodan, C. Radloff, N. J. Halas, P. Nordlander, *Science* **2003**, *302*, 419.
[36] S. J. Oldenburg, R. D. Averitt, S. L. Westcott, N. J. Halas, *Chem. Phys. Lett.* **1998**, *288*, 243.

